Fig. S1

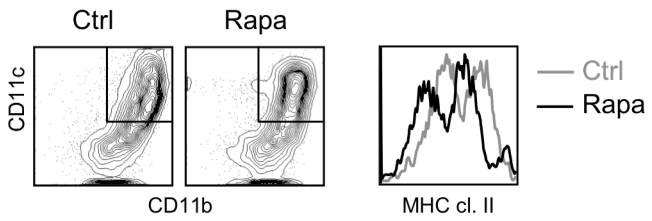

Figure S1. The effect of rapamycin on GM-CSF-driven DC development. Rapamycin (10 ng/ml) was added on day 0 to GM-CSF-supplemented cultures of wild-type BM. Shown are staining profiles on day 8, and the histograms of MHC cl. II expression in the gated $CD11c^+$ cDC (representative of 3 independent cultures). No reduction in the total cell output of rapamycin-treated cultures was noted (not shown).

Fig. S2

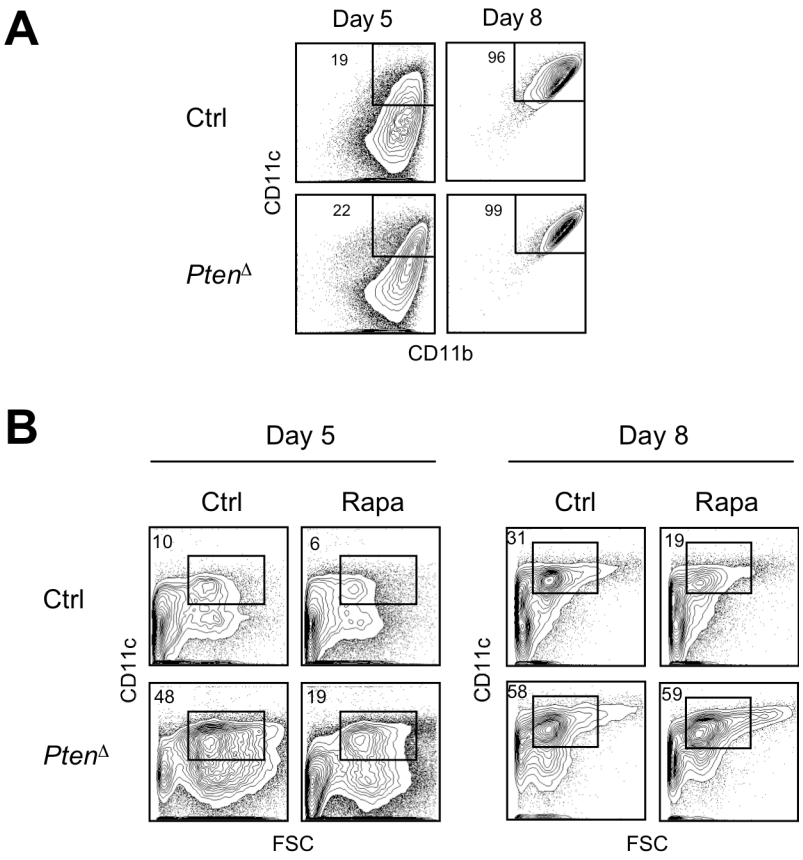

Figure S2. DC development from Pten-deficient bone marrow.

Pten deletion was induced by tamoxifen administration to *Pten*$^{fl/fl}$ *Gt(ROSA)26Sor*-CreER^{+} animals (*Pten*$^{\Delta}$) or littermate controls (Ctrl) as in Fig. 2.

(A) GM-CSF-driven DC development. Shown are staining profiles of GM-CSF-supplemented control and *Pten*$^{\Delta}$ BM cultures on days 5 and 8. No difference in the total cell output of the cultures was noted (not shown).

(B) The effect of rapamycin on Flt3L-driven DC development. Control and *Pten*$^{\Delta}$ BM cells were cultured with Flt3L in the presence or absence of 10 ng/ml rapamycin, and analyzed on days 5 and 8. Shown are staining profiles (representative of two independent experiments) with live CD11c^{+} DC highlighted.

Fig. S3

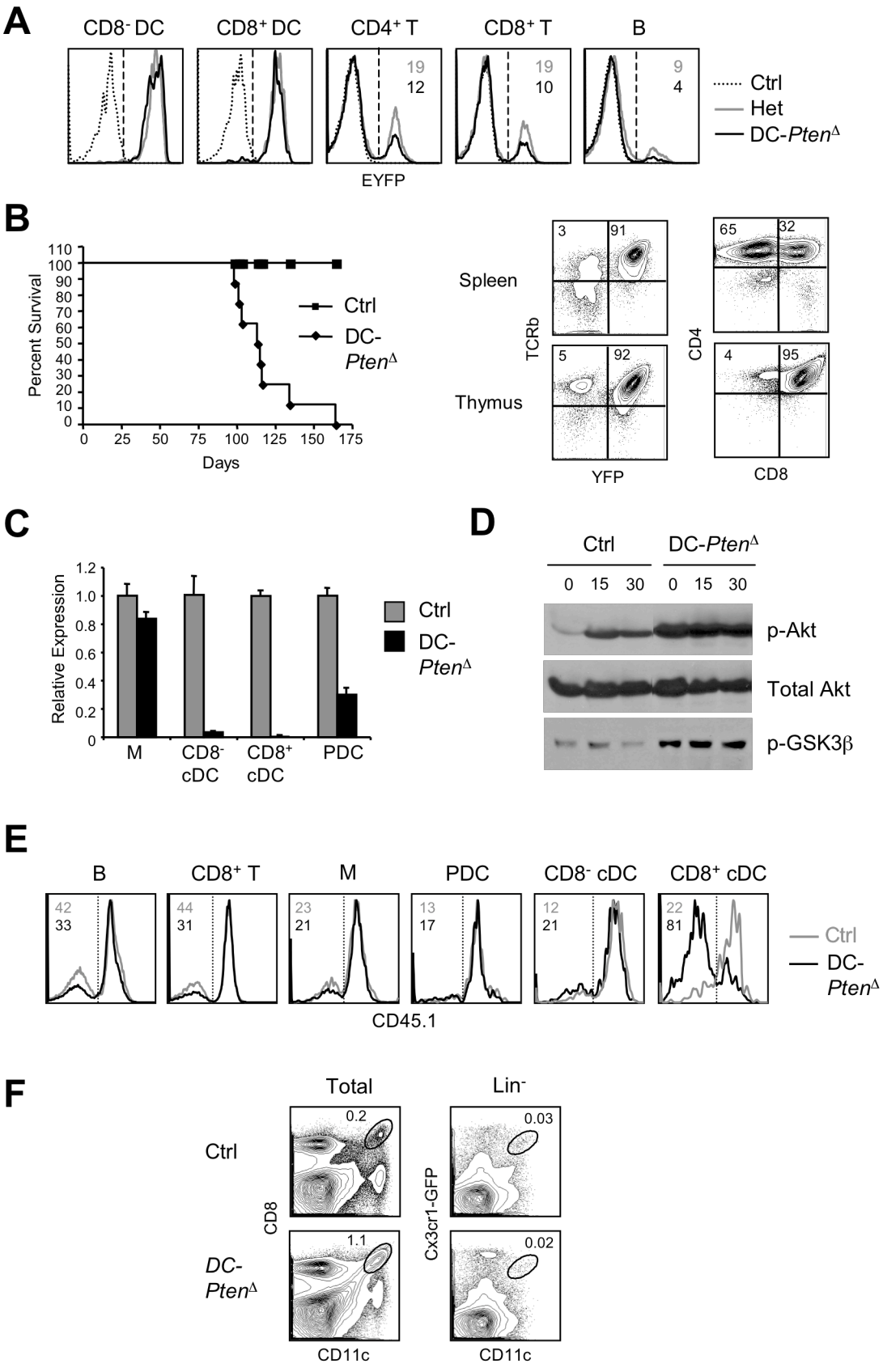
A
CD8- DC
CD8+ DC
CD4+ T
CD8+ T
B
19
12
19
10
9
4
Ctrl
Het
DC-Pten Δ
EYFP
B
Percent Survival
Days
Ctrl
DC-Pten Δ
Spleen
Thymus
TCRb
YFP
CD4
CD8
3
91
5
92
65
32
4
95
C
Relative Expression
M
CD8- cDC
CD8+ cDC
PDC
Ctrl
DC-Pten Δ
D
Ctrl
DC-Pten Δ
0 15 30 0 15 30
p-Akt
Total Akt
p-GSK3β
E
B
CD8+ T
M
PDC
CD8- cDC
CD8+ cDC
42
33
44
31
23
21
13
17
12
21
22
81
Ctrl
DC-Pten Δ
CD45.1
F
Total
Lin-
Ctrl
DC-Pten Δ
CD8
Cx3cr1-GFP
0.2
1.1
0.03
0.02
CD11c
CD11c

Figure S3. Characterization of DC-specific Pten deletion.

Pten$^{fl/fl}$ *Itgax*-Cre^{+} animals (DC-*Pten*$^{\Delta}$) and control *Itgax*-Cre^{-} littermates were analyzed.

(A) The specificity of Cre recombination in DC-*Pten*$^{\Delta}$ animals crossed with the Cre-inducible *Gt(ROSA)26Sor*-StopFlox-EYFP allele (Srinivas et al., 2001). Shown are histograms of EYFP fluorescence in the CD11c^{hi} MHC cl. II^{+} cDC subsets, T or B lymphocytes from *Gt(ROSA)26Sor*-StopFlox-EYFP^{+} Cre-negative (Ctrl), *Itgax*-Cre^{+} *Pten* heterozygous (*Pten*$^{fl/wt}$, Het) or *Itgax*-Cre^{+} *Pten*$^{fl/fl}$ (DC-*Pten*$^{\Delta}$) animals.

(B) Age-dependent development of T cell lymphomas in DC-*Pten*$^{\Delta}$ mice. Shown is Kaplan-Meyer survival plot of the DC-*Pten*$^{\Delta}$ and littermate control mice. On necropsy all DC-*Pten*$^{\Delta}$ mice showed a large thymic mass in the mediastinum, splenomegaly and lymphadenopathy. Flow cytometry plots represent the analysis of a moribund *Gt(ROSA)26Sor*-StopFlox-EYFP^{+} DC-*Pten*$^{\Delta}$ mouse, showing a recombined EYFP^{+} double-positive T cell lymphoma.

(C) The expression of *Pten* mRNA in monocytes or macrophages (M, side scatter^{lo} CD11c^{-} CD11b^{+}), cDC (CD11c^{hi} MHC cl. II^{+} CD8^{+} or CD8^{-}) or PDC (CD11c^{lo} Bst2^{+}) from DC-*Pten*$^{\Delta}$ or control (Ctrl) mice. Shown are normalized quantitative RT-PCR results relative to the expression value in control monocytes (mean ± S.D. of triplicate reactions). RT-PCR was performed using SYBR Green method with primers specific for Pten exon deleted after Cre recombination: 5'-TGGATTCAAAGCATAAAAACCATTAC-3' and 5'- CAAAAGGATACTGTGCAACTCTGC-3'.

(D) Western blot analysis of PI3K signaling in BM-derived cDC. GM-CSF-supplemented BM cultures from control and DC-*Pten*$^{\Delta}$ mice were left untreated (0) or stimulated with 1 μg/ml LPS for 15 or 30 min., and analyzed using antibodies against phosphorylated Akt

Ser473 and GSK3β Ser9 (Cell Signaling Technology). Note the constitutive Akt and GSK3β phosphorylation in untreated DC-*Pten*$^{\Delta}$ DC.

(E) Donor contribution to different cell types of chimeric mice. Irradiated CD45.1^{+} recipients were reconstituted with CD45.2^{+} DC-*Pten*$^{\Delta}$ or control donor BM and CD45.1^{+} competitor BM. Shown are representative CD45.1 expression profiles in the indicated splenic cell types, with the fraction of CD45.1^{-} donor-derived cells indicated. Note the substantial (~30-45%) donor contribution in lymphocytes, poor (15-20% contribution in myeloid cells and an overwhelming (>80%) contribution of DC-*Pten*$^{\Delta}$ but not control donor cells to CD8^{+} cDC.

(F) Splenic pre-DC after DC-specific Pten deletion. Control or DC-*Pten*$^{\Delta}$ mice carrying the *Cx3cr1*-EGFP knock-in reporter allele were analyzed. Shown is the CD8^{+} cDC population among total splenocytes (left), and the Cx3cr1^{hi} CD11c^{lo} pre-cDC population among the gated lineage-negative (MHC II^{-} CD11b^{-} Gr-1^{-} CD8^{-}) cells. Percentages out of total splenocytes are indicated. Additional staining for pre-DC markers Flt3 and CD115 confirmed equal fraction of pre-DC in control and DC-*Pten*$^{\Delta}$ spleens (not shown).

Fig. S4

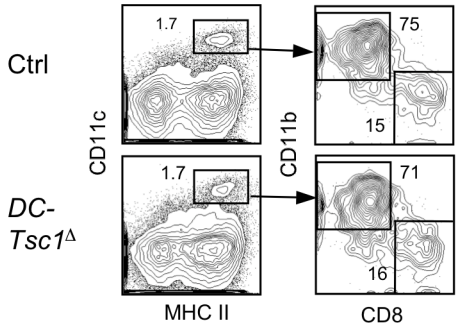

Figure S4. DC populations in mice with DC-specific deletion of Tsc1

Tsc1 conditional strain (Kwiatkowski et al., 2002) obtained from Jackson Labs was used for DC-specific targeting in *Tsc1*$^{fl/fl}$ *Itgax*-Cre^{+} (DC-*Tsc1*$^{\Delta}$) animals. Shown are staining profiles of splenic DC in the DC-*Tsc1*$^{\Delta}$ and Cre-negative littermate control mice (representative of three animals per genotype). Note the lack of CD8^{+} cDC expansion in DC-*Tsc1*$^{\Delta}$ mice.

Fig. S5

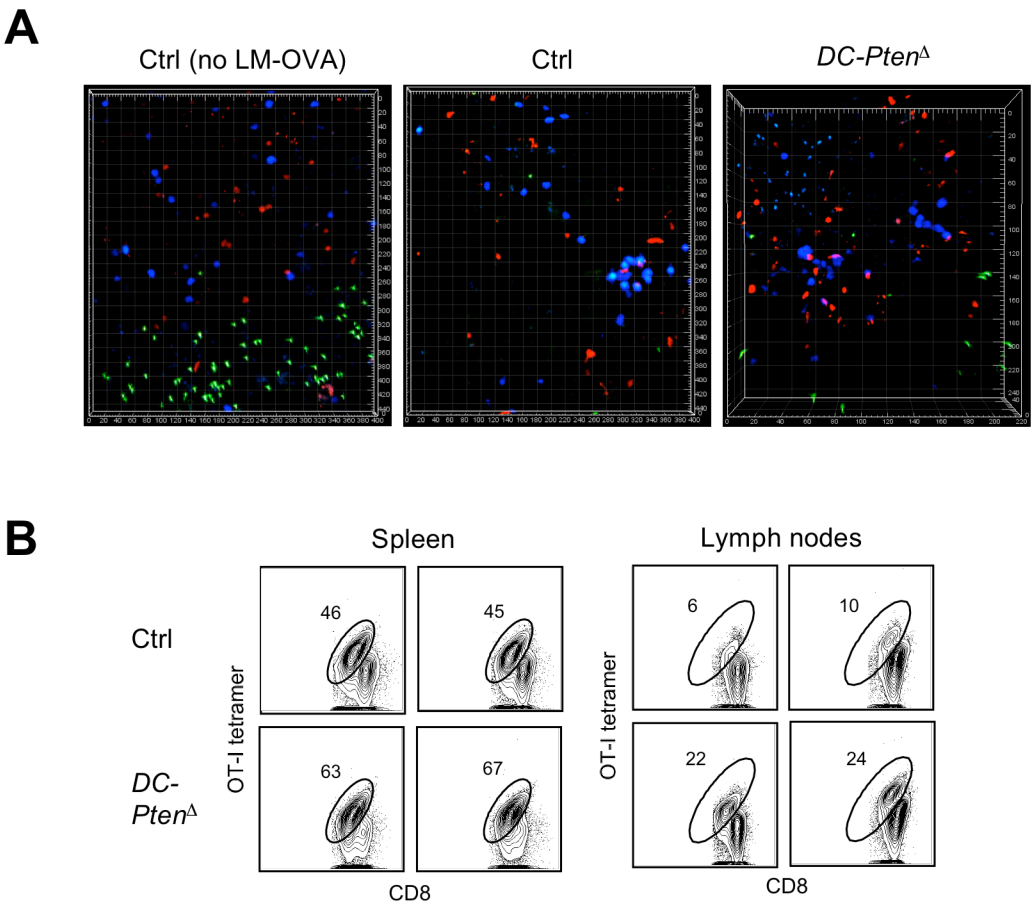

Figure S5. T cell response to LM-OVA in DC-*Pten*$^{\Delta}$ mice.

(A) Clustering of OVA-specific T cells in the early phase of LM-OVA infection. Splenic CD8^{+} T cells were isolated from OVA-specific OT-I TCR transgenic mice or from wild-type C57BL/6 mice and labeled with Cell Tracker (Invitrogen) Blue and Orange dyes, respectively. Labeled T cells were transferred (2x10^{6}/animal i.v.) into DC-*Pten*$^{\Delta}$ or control animals six hours prior to infection with 10^{5} LM-OVA. After 24 hr spleens were imaged by multiphoton microscopy as described (Aoshi et al., 2008). Shown are representative still images of OVA-specific (blue) and non-specific polyclonal (red) CD8^{+}

T cells from uninfected control, infected control or two infected DC-*Pten*$^{\Delta}$ animals. Note the prominent clustering of OVA-specific T cells in all infected animals.

(B) Expansion of OVA-specific T cells following LM-OVA infection. Splenic CD8^{+} T cells from OVA-specific OT-I TCR transgenic mice were transferred to DC-*Pten*$^{\Delta}$ or control animals (10^{6}/animal i.v.) 24 hours prior to infection with $2x10^{4}$ LM-OVA. Six days later, spleen and lymph nodes were analyzed for the presence of OT-I TCR-expressing T cells by flow cytometry. Shown are staining profiles from two control and DC-*Pten*$^{\Delta}$ animals. Similarly, no difference in the endogenous OVA-specific CD8^{+} T cell expansion was observed between control and DC-*Pten*$^{\Delta}$ animals (not shown).

Supplemental References

Aoshi, T., Zinselmeyer, B.H., Konjufca, V., Lynch, J.N., Zhang, X., Koide, Y., and Miller, M.J. (2008). Bacterial entry to the splenic white pulp initiates antigen presentation to CD8+ T cells. Immunity *29*, 476-486.

Kwiatkowski, D.J., Zhang, H., Bandura, J.L., Heiberger, K.M., Glogauer, M., el-Hashemite, N., and Onda, H. (2002). A mouse model of TSC1 reveals sex-dependent lethality from liver hemangiomas, and up-regulation of p70S6 kinase activity in Tsc1 null cells. Hum Mol Genet *11*, 525-534.

Srinivas, S., Watanabe, T., Lin, C.S., William, C.M., Tanabe, Y., Jessell, T.M., and Costantini, F. (2001). Cre reporter strains produced by targeted insertion of EYFP and ECFP into the ROSA26 locus. BMC Dev Biol *1*, 4.